Contribution from the Departments of Chemistry and Physics, Emory University, Atlanta, Georgia 30322

Nickel(II) Porphyrin Binding to Anionic Biopolymers Investigated by Resonance Raman and Optical Spectroscopy

K. T. Yue,*,‡ Mengfen Lin,† Thomas A. Gray,† and Luigi G. Marzilli*,†

Received January 15, 1991

Metalloporphyrins possess activity against HIV-1, the virus responsible for AIDS. In addition, some porphyrins with cationic charge also have anticancer activity and are interesting probes of nucleic acid properties. Ni(II) derivatives of *meso*-tetrakis(4-*N*-methylpyridiniumyl)porphyrin, NiTMpyP(4), and *meso*-tetrakis(2-*N*-methylpyridiniumyl)porphyrin, NiTMpyP(2), are particularly useful for study. In an aqueous solution, these nickel porphyrins exist in a six-(diaqua) to four-coordinate equilibrium mixture. The equilibrium position is dependent on the environment and on polymer binding. Resonance Raman spectroscopy is an especially powerful means for assessing this equilibrium because well-defined bands exist for each form. The utility of the resonance Raman method is enhanced when it is used in conjunction with optical spectroscopy. Resonance Raman studies have previously focused on porphyrin binding to double-stranded DNA. We have now extended the application of the method to other types of polymers, including single-stranded DNA and RNA, polypeptides, and sulfated carbohydrates. Resonance Raman studies from the Nakamoto laboratory have revealed that, except for $[poly(dAdT)]_2$, a relatively unperturbed four-coordinate form of NiTMpyP(4) dominated for duplex DNA bound forms at all ratios (R) of porphyrin to polymer. We find that this relatively unperturbed four-coordinate form predominates with the newly investigated polymers also. Typically, six-coordinate NiTMpyP(4) is not bound to polymers. However, we found that, at high R values, an unperturbed six-coordinate form of NiTMpyP(4) is bound to poly(U), poly(dU), and dextran sulfate. Our studies allow us to classify the various polymers based on their effectiveness in converting the six-coordinate forms of NiTMpyP(4) and NiTMpyP(2) to the respective four-coordinate forms. Nakamoto reported that a unique, perturbed four-coordinate species formed with $[poly(dAdT)]_2$ at 0.2 M NaCl. Our $[poly(dAdT)]_2$ studies were conducted at a relatively low salt concentration (0.01 M NaCl). New CD and absorption spectroscopic studies under both conditions reveal that the low salt conditions promote the formation of a previously unrecognized spectroscopically distinct form of NiTMpyP(4) bound to $[poly(dAdT)]_2$ at high R. Our evidence that this species may involve porphyrin-porphyrin stacking includes a hypochromic effect in the absorption spectrum and a conservative CD spectrum in the Soret region. At lower R values or at all R values at higher salt, this stacked species was not observed. Instead, the spectra were similar, with a hyperchromic Soret band and a less conservative CD spectrum dominated by a positive band at ca. 415 nm. Although the optical spectra were different, the broadening of the Raman spectral band at ca. 1097 cm^{-1}, characteristic of the unique four-coordinate species, was observed in both cases. The $[poly(dAdT)]_2$ polymer is weakly stacked, with an unhindered minor groove. The weak stacking leads to flexibility. Apparently, flexibility is not sufficient to induce the formation of the unique four-coordinate form of NiTMpyP(4), since the broadening of the ca. 1097-cm^{-1} band was not observed with either the single-stranded nucleic acids or the other polymers studied here. Formation of the unique species identified by resonance Raman spectroscopy may require interaction of the porphyrin with an unhindered minor groove in a duplex.

Introduction

The interaction of water-soluble porphyrins and metalloporphyrins with DNA has attracted considerable recent interest.[1-4] There are three main reasons for this interest. First, the two basic modes of porphyrin binding to DNA—intercalation and outside binding—can be used as models for the DNA binding of anticancer drugs.[4,5] Second, certain porphyrins are photosensitizers and can be useful in the photodynamic therapy of cancer.[6-9] This therapy likely depends on the damage caused to DNA during photolysis. Third, evidence exists that porphyrins can inhibit HIV-1, the virus responsible for AIDS.[10,11] Understanding the modes of the binding of porphyrins to DNA and the factors that can affect the binding is of fundamental importance in understanding DNA binding in general. Typically, intercalation involves a relatively hydrophobic, polar, planar region of the DNA binder, but electrostatic, dipole–dipole, and H-bonding interactions between the intercalator and DNA are also important.[12,13] On the other hand, outside binding is favored by these electrostatic and H-bonding interactions, and hydrophobic effects are less important. Furthermore, steric hindrance or a lack of planarity close to the planar region inhibits intercalation, thereby favoring outside binding.

Until recently, the majority of reports on porphyrin–DNA interactions had concentrated on *meso*-tetrakis(4-*N*-methylpyridiniumyl)porphyrin (TMpyP(4), Figure 1) and its metal derivatives. Lately, studies on other cationic porphyrins have been reported.[1,3,14,15] Many physicochemical and biochemical techniques have been employed to study these interactions.[1-4,12-26] It is generally believed that TMpyP(4) intercalates specifically into GC-containing sequences at 5′-CG sites, whereas outside binding occurs for AT-containing sequences.[4,16,17,24] Metal complexes of TMpyP(4) with no axial ligands or weak axial ligands such as Ni(II), Cu(II), or Au(III) can also intercalate at GC sites.[4,21] Nakamoto and his group have shown that soluble TMpyP(4)

† Department of Chemistry.
‡ Department of Physics.

(1) Sari, M. A.; Battioni, J. P.; Dupré, D.; Mansuy, D.; Le Pecq, J. B. *Biochemistry* **1990**, *29*, 4205-4215.
(2) Groves, J. T.; Farrell, T. P. *J. Am. Chem. Soc.* **1989**, *111*, 4998-5000.
(3) Slama-Schwok, A.; Lehn, J.-M. *Biochemistry* **1990**, *29*, 7895-7903.
(4) Marzilli, L. G. *New J. Chem.* **1990**, *14*, 409-420.
(5) Waring, M. J. *Annu. Rev. Biochem.* **1981**, *50*, 159-192. Wilson, W. D.; Jones, R. L. In *Intercalation Chemistry*; Whittingham, M. S., Jacobson, A. J., Eds.; Academic Press: New York, 1982; pp 445-501.
(6) Musser, D. A.; Datta-Gupta, N.; Fiel, R. J. *Biochem. Biophys. Res. Commun.* **1980**, *97*, 918-925.
(7) Fiel, R. J.; Datta-Gupta, N.; Mark, E. H.; Howard, J. C. *Cancer Res.* **1981**, *41*, 3543-3545.
(8) Praseuth, D.; Gaudemer, A.; Verlhac, J.-B.; Kraljic, I.; Sissoeff, I.; Guille, E. *Photochem. Photobiol.* **1986**, *44*, 717-724.
(9) Villanueva, A.; Hazen, M. J.; Stockert, J. C. *Experientia* **1986**, *42*, 1269-1271.
(10) Dixon, D. W.; Marzilli, L. G.; Schinazi, R. *Ann. N.Y. Acad. Sci.* **1990**, *611*, 511-513.
(11) Sessler, J. L.; Cyr, M. J.; Lynch, V. *J. Am. Chem. Soc.* **1990**, *112*, 2810-2813.
(12) Strickland, J. A.; Marzilli, L. G.; Gay, K. M.; Wilson, W. D. *Biochemistry* **1988**, *27*, 8870-8878.
(13) Strickland, J. A.; Marzilli, L. G.; Wilson, W. D.; Zon, G. *Inorg. Chem.* **1989**, *28*, 4191-4198.
(14) Bütje, K.; Nakamoto, K. *J. Inorg. Biochem.* **1990**, *39*, 75-92.
(15) Gray, T. A.; Yue, K. T.; Marzilli, L. G. *J. Inorg. Biochem.* **1991**, *41*, 205-219.
(16) Fiel, R. J. *J. Biomol. Struct. Dyn.* **1989**, *6*, 1259-1274.
(17) Gibbs, E. J.; Pasternack, R. F. *Semin. Hematol.* **1989**, *26*, 77-85.
(18) Geacintov, N. E.; Ibanez, V.; Rougee, M.; Bensasson, R. V. *Biochemistry* **1987**, *26*, 3087-3092.
(19) Kelly, J. M.; Murphy, M. J.; McConnell, D. J.; OhUigin, C. *Nucleic Acids Res.* **1985**, *13*, 167-184.
(20) Dougherty, G.; Pilbrow, J. R.; Skorobogaty, A.; Smith, T. D. *J. Chem. Soc., Faraday Trans. 2* **1985**, *81*, 1739-1759.
(21) Strickland, J. A.; Banville, D. L.; Wilson, W. D.; Marzilli, L. G. *Inorg. Chem.* **1987**, *26*, 3398-3406.
(22) Strickland, J. A.; Marzilli, L. G.; Wilson, W. D. *Biopolymers* **1990**, *29*, 1307-1323.

0020-1669/91/1330-3214$02.50/0

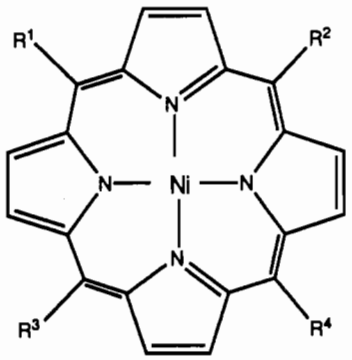

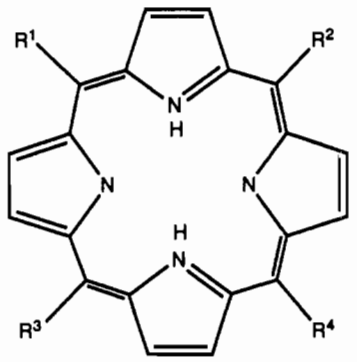

NiTMpyP(4): $R^1 = R^2 = R^3 = R^4 =$ 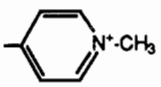

TMpyP(4): $R^1 = R^2 = R^3 = R^4 =$ 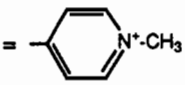

NiTMpyP(2): $R^1 = R^2 = R^3 = R^4 =$ 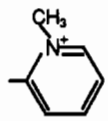

Figure 1. Structure of porphyrins referred to in the present study.

and related porphyrins with Cu(II), Ni(II), and Co(III) can be studied by resonance Raman spectroscopy.[25] They further suggested that characteristic changes observed when these soluble porphyrins bind to different DNA polymers are indicative of the DNA binding mode.[14,23,26] These comprehensive studies from the Nakamoto laboratory have demonstrated the great power of resonance Raman spectroscopy to study DNA binding of porphyrins. In most other cases, DNA binding drugs do not undergo enough structural change to make assessment of drug binding by analysis of the vibrational spectrum of the drug useful; in these cases, insight can be gained by utilizing the vibrational bands of DNA.

One of the water-soluble metalloporphyrins, NiTMpyP(4), is of particular interest. It is a mixture of a four-coordinate form and a diaqua, six-coordinate form in aqueous solution. The ratio of four- to six-coordination can be shifted by adding acetone, indicating that this ratio is sensitive to the environment of the porphyrins.[27] The two forms have different Soret peak intensities and positions in the visible absorption spectrum; the four-coordinate species has a peak at 418 nm, whereas the diaqua form has a peak at 440 nm. Pioneering optical studies of this porphyrin have contributed significantly to our understanding of the binding of cationic porphyrins to DNA.[28] However, these visible absorptions are broad and overlapping, features that limit their use in monitoring the ratio of the two forms. In addition, changes in intensity and position of the Soret bands upon binding to DNA can also complicate the analysis of this ratio. Such electronic spectral changes are also sensitive to small changes in the environment of the porphyrin.

On the other hand, the characteristic Raman bands associated with each form of NiTMpyP(4)[25] can be used to monitor more directly changes in the ratio. Since only the four-coordinate form can intercalate, disappearance of the Raman bands associated with the six-coordinate species upon binding to calf thymus DNA was expected.[25] However, later reports demonstrated that these six-coordination bands also disappear upon binding to AT regions.[14,23,26] In addition, other more subtle changes in the Raman spectra of porphyrins upon binding to different DNA polymers were mentioned. Questions remain as to the exact nature of the binding of NiTMpyP(4) to different DNAs, especially in the AT-rich regions. Recently, Nakamoto and his group have extended these studies to other porphyrins, including nickel *meso*-tetrakis(2-*N*-methylpyridiniumyl)porphyrin (NiTMpyP(2), Figure 1). NiTMpyP(2) also exists in four- and six-coordinate forms[29] characterized by 410- and 428-nm Soret bands, respectively. However, it is known to be unable to intercalate into DNA because of steric hindrance.[21,29]

In this paper, we report new resonance Raman, visible absorption and CD spectral studies of the binding of NiTMpyP(4) and NiTMpyP(2) to (a) the non-double-helical nucleic acids poly(dU) and poly(U); (b) other anionic, non nucleic acid polymers, including dextran sulfate, heparin, phosvitin, and poly(D-glutamic acid); and (c) the DNA duplexes calf thymus DNA [CT DNA], poly(dA-dT)·poly(dA-dT) [[poly(dAdT)]$_2$], and poly(dG-dC)·poly(dG-dC) [[poly(dGdC)]$_2$]. The DNA duplexes were investigated previously, but we have used low salt conditions in this study, which allowed us to detect even weak interactions. We have found that the ratio of four- to six-coordinate nickel is indeed sensitive to the environment and can be used to provide information on the nature of the binding modes and binding sites of these nickel porphyrins to other diverse polymers. Furthermore, this ratio is sensitive to different ranges of electrostatic interactions for the two nickel porphyrins.

Experimental Section

PIPES buffer [0.01 M PIPES (piperazine-*N*,*N*′-bis[2-ethanesulfonic acid], Sigma), 10^{-5} M EDTA (ethylenediaminetetraacetic acid, Aldrich), deionized water] containing no salt (PIPES 00) was adjusted to pH 7.00 with aqueous NaOH and passed through a 0.22-μm millipore filter. CT DNA was obtained from Worthington. [Poly(dAdT)]$_2$, [poly(dGdC)]$_2$, poly(U), and poly(dU) were obtained from Pharmacia. All DNAs were unsonicated and were prepared and stored in PIPES 00 buffer or 0.01 M NaCl solution. Extinction coefficients used to determine the polynucleotide concentrations in base pairs were as follows: CT DNA, $\epsilon_{260} = 1.32 \times 10^4$ M^{-1} cm^{-1};[30] [poly(dAdT)]$_2$, $\epsilon_{262} = 1.32 \times 10^4$ M^{-1} cm^{-1};[31]

(23) Schneider, J. H.; Odo, J.; Nakamoto, K. *Nucleic Acids Res.* **1988**, *16*, 10323–10338.
(24) Marzilli, L. G.; Banville, D. L.; Zon, G.; Wilson, W. D. *J. Am. Chem. Soc.* **1986**, *108*, 4188–4192.
(25) Blom, N.; Odo, J.; Nakamoto, K. *J. Phys. Chem.* **1986**, *90*, 2847–2852.
(26) Bütje, K.; Schneider, J. H.; Kim, J.-J. P.; Wang, Y.; Ikuta, S.; Nakamoto, K. *J. Inorg. Biochem.* **1989**, *37*, 119–134.
(27) Pasternack, R. F.; Spiro, E. G.; Teach, M. *J. Inorg. Nucl. Chem.* **1974**, *36*, 599–606.
(28) Pasternack, R. F.; Gibbs, E. J.; Villafranca, J. J. *Biochemistry* **1983**, *22*, 2406–2414.
(29) Bütje, K.; Nakamoto, K. *Inorg. Chim. Acta* **1990**, *167*, 97–108.

$[poly(dGdC)]_2$, $\epsilon_{254} = 1.68 \times 10^4$ M^{-1} cm^{-1}.[32] The extinction coefficient used for poly(dU) and poly(U) per base was $\epsilon_{260} = 9 \times 10^3$ M^{-1} cm^{-1}.[33]

Dextran sulfate, heparin, phosvitin and poly(D-glutamic acid) were obtained from Sigma and used without further purification. The concentration of charged units, e.g. sulfate in dextran sulfate, was used to calculate the ratios given below. The following values were used: dextran sulfate ($-OSO_3^-$), 5.3×10^{-3} mol/g; heparin ($-CO_2^-$, $-OSO_3^-$), 5.2×10^{-3} mol/g; phosvitin (OPO_3^{2-}), 3.3×10^{-3} mol/g; poly(D-glutamic acid) ($-CO_2^-$), 7.5×10^{-3} mol/g. These values were obtained by calculations based on polymer compositions obtained from either elemental analysis or structural considerations. For example phosvitin is stated to be 10% P by weight.[34] Similarly, dextran sulfate is stated to be 17% sulfate by weight.[35] Calculations for heparin and poly(D-glutamic acid) required some assumptions: the average structural unit was ascertained.[36,37] The number of anionic sites in each unit was calculated and converted into the number of moles of anionic sites per gram.

Chloride salts of NiTMpyP(4) and NiTMpyP(2) (Figure 1) were obtained from Midcentury. Porphyrins were purified by gel filtration chromatography, using Sephadex LH-20 as the stationary phase and a 1:1 solution of methanol and either 0.01 M aqueous $NaHCO_3$ or 0.01 M aqueous KH_2PO_4 as the eluant. The purity was then checked by gel electrophoresis. The extinction coefficient for NiTMPyP(2) ($\epsilon_{428} = 2.0 \times 10^5$ M^{-1} cm^{-1}) was determined by titrating a quartz cell containing deionized water with a stock solution of the dried porphyrin in deionized water. Beer's law was followed during the titration. The extinction coefficient for NiTMpyP(4) ($\epsilon_{418} = 1.5 \times 10^5$ M^{-1} cm^{-1}) was determined in previous work.[27]

Visible spectral experiments were conducted with an Aviv Model 14DS spectrophotometer. Typically, 5–10 μL of porphyrin stock solution (≈1.0 mM) was added to 0.25 mL of 0.01 M NaCl in a 1-mm-path quartz UV cell (the total cell volume was 0.30 mL). The absorption spectrum of the porphyrin solution (typically ca. 30 μM) was then recorded in the 600–350-nm range. Then aliquots of a stock DNA solution CT DNA, $[poly(dAdT)]_2$, $[poly(dGdC)]_2$ (ca 3×10^{-3} M in base pairs), or poly(dU) (ca. 6×10^{-3} M in bases) in 0.01 M NaCl were added and the spectrum measured after each addition until a porphyrin/DNA base pair ratio, R, of ≤0.05 (or base ratio ≤0.025) was achieved at the end of the titration. Alternatively, the same amount of porphyrin stock (≈5 μL, 1.9×10^{-5} M final concentration) was added to a polymer solution (0.013 g of dextran sulfate, heparin, phosvitin or poly(D-glutamic acid) in 0.25 mL 0.01 M NaCl), and the spectrum was recorded. In the dextran sulfate and poly(U) titrations, the porphyrin concentrations used were $(3.6–3.8) \times 10^{-5}$ M for NiTMpyP(4) and 2.8×10^{-5} M for NiTMpyP(2).

Circular dichroism (CD) spectra were recorded on a JASCO 600 spectropolarimeter. Porphyrin solutions, typically 2.0×10^{-5} M, were contained in a 5 mm path length quartz cell. Titrations were performed as described above for the visible spectral studies.

Raman measurements were done with the samples (ca. 1 to 5×10^{-5} M) in melting point capillaries. The typical concentration of porphyrin was 30 μM. Either an argon ion laser (Spectra Physics Model 164 or Model 2025) or a krypton ion laser (Coherent Innova 100) was used for excitations. Power at the samples was kept below 20 mW. Raman signals were collected via a 90° geometry by a triple monochromator (Spex Model 1877 triplemate) and one of two photodiode array detector systems: an EG&G OMA III system consisting of a Model 1420 detector and a Model 1460 controller or a Model IRY-1024 detector and a Model ST-120 controller from Princeton Instruments. Calibrations for the OMA systems were performed for each measurement by using known Raman lines of toluene. Peak positions are accurate to within ±2 cm^{-1} between different runs. Typical resolution is 6–10 cm^{-1}. Spectra were transferred, stored, and analyzed with an AT-compatible microcomputer. No changes (both spectral features and intensities) in the Raman spectra as a function of exposure time to the laser were observed for all the samples studied.

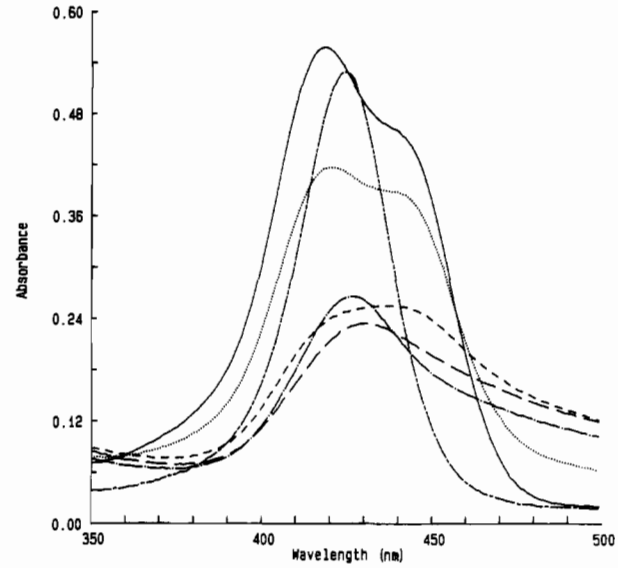

Figure 2. Visible spectral titration of NiTMPyP(4) (3.6×10^{-5} M) (—) with poly(U), in 0.01 M NaCl, pH 7.0: $R = 0.5$ (···); $R = 0.25$ (- - -); $R = 0.2$ (– –); $R = 0.1$ (–·–); $R = 0.01$ (–·–·–).

Results

UV–Visible Spectroscopy. The effects of solvent, salt concentration, and polymers on the relative amounts of four- and six-coordinate NiTMpyP(4) and NiTMpyP(2) were assessed by monitoring the Soret spectral region (cf. Figure 2, below). The spectrum is sensitive to solvent conditions but generally has a band at 418 nm for the four-coordinate form and a shoulder at ca. 440 nm for the six-coordinate form. It is known that addition of aceteone to a solution of NiTMpyP(4) in deionized water greatly decreases the intensity of the 440-nm shoulder.[27] We noted that acetone also caused hyperchromicity and a slight blue shift in the ca. 418-nm band of the four-coordinate porphyrin. For example, between 30% and 60% acetone, the band shifted ca. 2 nm with a 10% increase in intensity. However, we found that the addition of NaCl (to 1.0 M NaCl) to a solution of NiTMpyP(4) in deionized water produced very little change in the visible spectrum of the nickel porphyrin (cf. figures below). There was a very slight increase (<5%) in the intensity of the 440-nm band at the expense of the 418-nm band. Similar, very small changes were observed in the spectrum of NiTMpyP(2) upon addition of NaCl.

The presence of CT DNA, $[poly(dAdT)]_2$, or $[poly(dGdC)]_2$ in a 0.01 M NaCl solution of NiTMpyP(4) resulted in the complete disappearance of the band at 440 nm corresponding to the six-coordinate species when R ([porphyrin]/[base pairs] for duplexes) was decreased to less than ca. 0.25. High DNA concentrations affected the 418-nm band of NiTMpyP(4) in a manner consistent with intercalation into CT DNA and $[poly(dGdC)]_2$ (intensity decreases of 20–30% and red shifts of 10–20 nm) or surface binding for $[poly(dAdT)]_2$ (intensity increase and a small red shift); see ref 15 and 28 for similar experiments at other conditions.

The NiTMpyP(4) solutions containing $[poly(dAdT)]_2$ are of particular interest in view of the CD and Raman results. Therefore, an extensive study was undertaken with both low (0.01 M) and high (0.2 M) concentrations of NaCl. In both cases, the final spectral changes were similar to each other and those reported previously.[15,28] Namely, we observed a 4-nm red shift and intensity increases of 23 and 28% for low and high salt concentrations, respectively. However, at high R values, less porphyrin appeared to be bound at high salt concentrations, as expected, and there was an initial decrease in the Soret band for the low salt conditions down to R = ca. 0.5.

In contrast, addition of either poly(dU) or poly(U) to a solution of NiTMpyP(4) had a very *different* effect on the bands in the visible spectrum (Figure 2). The addition of poly(U) to a NiTMpyP(4) solution (3.6×10^{-5} M) decreased the intensities of the 418-nm band and the ca. 440-nm shoulder, with the former

(30) Wells, R. D.; Larson, J. E.; Grant, R. C.; Shortle, B. E.; Cantor, C. R. *J. Mol. Biol.* **1970**, *54*, 465–497.
(31) Schmechel, D. E. V.; Crothers, D. M. *Biopolymers* **1971**, *10*, 465–480.
(32) Muller, W.; Crothers, D. M. *J. Mol. Biol.* **1968**, *35*, 251–290.
(33) Torrence, P. F.; De Clercq, E.; Witkop, B. *Biochemistry* **1976**, *15*, 724–734.
(34) Belitz, H.-D. *Angew. Chem., Int. Ed. Engl.* **1964**, *3*, 645.
(35) *Merck Index*, 11th ed.; Merck & Co.: Rahway, NJ, 1989; No 2929, p 465.
(36) Lindahl, U.; Hook, M.; Bäckström, G.; Jacobsson, I.; Riesenfeld, J.; Malmström, A.; Rodén, L.; Feingold, D. S. *Fed. Proc.* **1977**, *36*, 19.
(37) *Merck Index*, 11th ed.; Merck & Co.: Rahway, NJ, 1989; No. 4363, p 702.
(38) Shamin, A.; Hambright, P. *Inorg. Chem.* **1980**, *19*, 564–566.

Table I. Effects of Anionic Polymers on the Soret Band of NiTMpyP(4) and NiTMpyP(2) at $R \approx 10^{-4}$

	NiTMpyP(4)			NiTMPyP(2)	
polymer	λ_{max}, nm	$(A^a/A^b)_{418}$, %	six-coordinate	$(A^c/A^b)_{410}$, %	$(A^c/A^b)_{428}$, %
dextran sulfate	424	124	none	210	55
phosvitin	422	105	slight amount	slight change	80
heparin	418	92	slight amount	slight change	102
poly(D-glutamic acid)	418	112	slight amount	100	100

[a] The absorbance of NiTMpyP(4) at the λ_{max} indicated. [b] Initial absorbance at λ indicated prior to the addition of polymer. [c] The absorbance of NiTMpyP(2) in the presence of polymer.

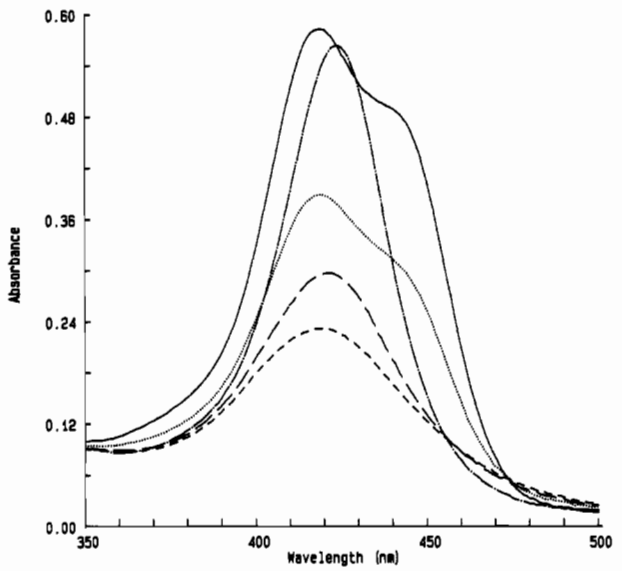

Figure 3. Visible spectral titration of NiTMpyP(4) (3.8×10^{-5} M) (—) with dextran sulfate, in 0.01 M NaCl, pH 7.0: $R = 0.5$ (···); $R = 0.2$ (- - -); $R = 0.125$ (– –); $R = 0.01$ (–·–).

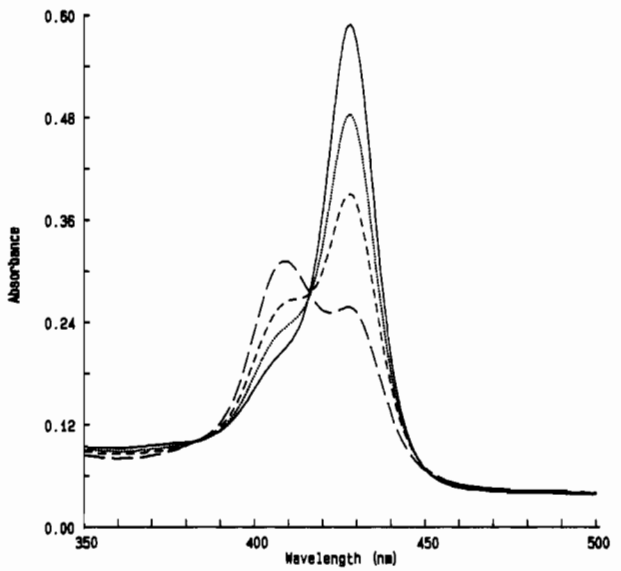

Figure 4. Visible spectral titration of NiTMpyP(2) (2.8×10^{-5} M) (—) with poly(U) in 0.01 M NaCl, pH 7.0: $R = 1.0$ (···); $R = 0.5$ (- - -); and $R = 0.25$ (– –).

decreasing more sharply. At about R ([porphyrin]/[base] for single-stranded nucleic acids) = 0.25, the shoulder and the 418-nm band were of about equal intensity and appeared as a broad combined band. At $R = 0.2$, the broad combined band reached its lowest intensity, which is only 38% of that of the original signal. At $R = 0.2$, the shoulder had essentially disappeared. At lower and lower R values, a symmetrical band at 424 nm became more and more prominent, reaching an intensity of ca. 92% of the original band in this region, at $R = 0.01$. Very similar results were found with poly(dU), suggesting that the unusual spectral changes are independent of the nature of the sugar.

Changes in the visible spectrum of NiTMpyP(4) in 0.01 M NaCl were also studied in the presence of the anionic polymers dextran sulfate, heparin, phosvitin and poly(D-glutamic acid) (R ca. 10^{-4}, Table I; R = [porphyrin]/[anionic unit] for non nucleic acid polymers). These polymers also decreased greatly the relative amounts of the four-coordinate porphyrin to the six-coordinate porphyrin (Table I).

Titration of NiTMpyP(4) with dextran sulfate (Figure 3) showed that addition of dextran sulfate caused a proportional decrease in the intensities of both bands, up to $R = 0.25$; the shoulder at ca. 440 nm disappeared at $R = 0.25$, and the intensity of the 418-nm band was only 37% of that of NiTMpyP(4) in 0.01 M NaCl. Continued addition of dextran sulfate, however, produced a symmetric band with a maximum absorbance at 424 nm, and the intensity of this band increased with the concentration of dextran sulfate. At $R = 0.01$ the intensity of the 424-nm band was 96% of that of the NiTMPyP(4) in 0.01 M NaCl. As a first approximation, the results with dextran sulfate, poly(dU), and poly(U) were very similar, especially at very low R values.

The visible spectrum of NiTMpyP(2) also has two bands in water (Figure 4), but the longer wavelength band for the six-coordinate form dominates. As found for NiTMPyP(4), 0.01 M NaCl has relatively little effect on the spectrum. An increasing percentage of acetone in a solution of NiTMpyP(2) also resulted in a decrease in the intensity of the band at 428 nm for the six-coordinate species, in general agreement with a previous report.[29]

Addition of $[poly(dAdT)]_2$, $[poly(dGdC)]_2$, poly(U), and CT DNA to NiTMpyP(2) reduced the ca. 428-nm band and increased the ca. 410-nm band to a different extent; $[poly(dAdT)]_2$ was the most effective and poly(U) the least effective. Of the four anionic polymers studied, only dextran sulfate caused significant changes in the Soret region of NiTMpyP(2); heparin and poly(D-glutamic acid) had no effect (Table I).

CD Spectroscopy. In the absence of polymers, NiTMpyP(4) had no CD signal, as expected. Addition of dextran sulfate to a NiTMpyP(4) solution (1.5×10^{-5} M) induced a negative CD signal at 428 nm. The ellipticity increased as the ratio R decreased. At $R = 0.01$, the molecular ellipticity was -3.5×10^4 deg cm^2 dmol^{-1}.

Addition of poly(U) to a NiTMpyP(4) solution induced a conservative CD signal in the initial stages ($R \geq 0.25$). At $R = 0.25$, the conservative CD signal was most pronounced; the negative (441 nm) and positive (417 nm) bands had molecular ellipticities of -2.8×10^4 and 6.6×10^3 deg cm^2 dmol^{-1}, respectively. With further addition of poly(U), the positive band disappeared and the negative band shifted. At $R = 0.05$ this band appeared at 432 nm, with a molecular ellipticity of -2.2×10^4 deg cm^2 dmol^{-1}.

The CD titrations of NiTMpyP(4) with $[poly(dAdT)]_2$ were performed in 0.01 and 0.2 M NaCl solution. In 0.01 M NaCl solution, with the addition of $[poly(dAdT)]_2$, a conservative CD signal was induced in the visible region with the positive signal at 437 nm and the negative signal at 419 nm (Figure 5). With increased $[poly(dAdT)]_2$, both signals increased. At $R = 0.38$, the conservative signal reached its maximum value, with molecular ellipticities of 3.3×10^5 and -1.5×10^5 deg cm^2 dmol^{-1}. At lower ratios, the conservative signal decreased and a positive band appeared at ca. 410 nm. At $R = 0.2$, an inverted conservative-like signal was obtained, with the negative signal at 428 nm and the positive signal at 409 nm. At very low R values, the negative CD

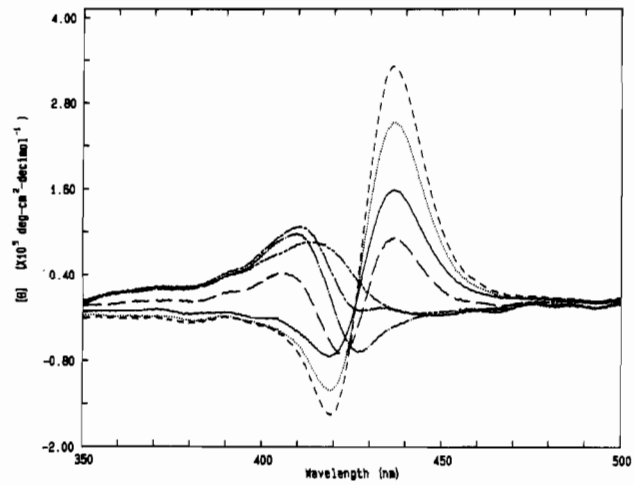

Figure 5. Induced circular dichroism spectra of NiTMpyP(4) (1.03×10^{-5} M) with $[poly(dAdT)]_2$ at pH 7.0 in 0.01 M NaCl: $R = 0.75$ (—); $R = 0.5$ (···); $R = 0.38$ (- - -); $R = 0.25$ (– –); $R = 0.2$ (– · –); $R = 0.15$ (– – –); $R = 0.05$ (– – – –).

band decreased and the positive band shifted to ca. 415 nm. In 0.2 M NaCl solution, the addition of $[poly(dAdT)]_2$ induced only the inverted conservative-like signal with a negative band at 440 nm and a positive one at 416 nm, at $R = 0.05$. The spectra (not shown) are similar to those obtained at $R < 0.15$ in 0.01 M NaCl.

Raman Spectroscopy. Nakamoto and his group have shown that Raman spectroscopy provides a very clean and unambiguous way to monitor the amount of six-coordinate NiTMpyP(4).[25] The advantage is amplified by the ability to selectively enhance each species by changing the excitation wavelength. The four-coordinate species has a 418-nm Soret band and its bands are selectively enhanced by 406.7-nm excitation. Likewise, the bands of the six-coordinate species (Soret at 440 nm) are enhanced by 457.9-nm excitation. The complete absence of a particular species can be demonstrated only by using the appropriate excitation wavelength. We found that using 457.9-nm excitation gave better results than the 406.7-nm excitation most often reported previously with NiTMpyP(4).

Typical spectra of NiTMpyP(4) in 0.01 M NaCl between 850 and 1700 cm^{-1} using 457.9- and 406.7-nm excitation, spectra a and b in Figure 6, respectively, clearly show that specific modes are selectively enhanced by the two different excitations. For example, peaks at ca. 1354, 1454, and 1558 cm^{-1}, are much stronger for 457.9-nm excitation, whereas the peaks at ca. 1376, 1478 and 1583 cm^{-1} are enhanced by 406.7-nm excitation. The corresponding peaks are either much weaker or disappear completely for the other excitation. For each coordination form, the three peaks mentioned for each excitation are due to core-size-sensitive C_α–N, C_α–C_β, and C_β–C_β stretches, respectively.[25] In addition, there are some subtle changes in the ca. 1003- and 1097-cm^{-1} peaks. When the excitation wavelength was changed from 457.9 to 406.7 nm, the ca. 1003-cm^{-1} peak width was broadened and its intensity was reduced while the intensity of the 1097-cm^{-1} peak was enhanced (cf. Figure 6 and ref 23). It is clear that both peaks are composed of two bands. One band is associated with the six-coordinate species and the other with the four-coordinate species. For example, with 457.9-nm excitation, the sharp peak at 1003 cm^{-1} is due mainly to a six-coordinate-related band. With 406.7-nm excitation, it is much weaker, whereas another weak band at a slightly higher frequency related to the four-coordinate species is enhanced to give a broader overall peak at 1009 cm^{-1}. Similarly, the ca. 1097-cm^{-1} peak with 457.9-nm excitation can be attributed to both four- and six-coordinate bands.

In agreement with a previous report,[23] when acetone was added, the six-coordinate species decreased. At about 50% acetone by volume, bands for the six-coordinate species were no longer evident. In addition, the peaks at ca. 1003 and 1097 cm^{-1} shifted to ca. 1007 and 1101 cm^{-1}, respectively, in 50% acetone with 457.9-nm

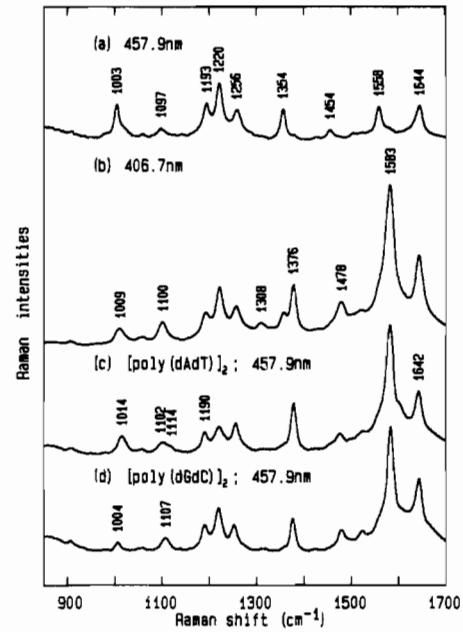

Figure 6. Raman spectra of NiTMpyP(4) with 457.9-nm excitation (a), with 406.7-nm excitation (b), with $[poly(dAdT)]_2$ and 457.9-nm excitation (c), and with $[poly(dGdC)]_2$ and 457.9-nm excitation (d). Concentrations of NiTMpyP(4) were 0.04, 0.04, 0.03, and 0.03 mM, respectively. Samples were at ambient temperature, in 0.01 M NaCl (pH 7.0). A smooth background has been subtracted for each spectrum.

excitation (data not shown). Although the bands of the six-coordinate form are still evident in the Raman spectrum in ca. 30% acetone, the Soret band for the six-coordinate form is not clearly evident, possibly because of the hyperchromicity of the four-coordinate Soret band in the mixed-solvent system.

In the Raman spectra of NiTMpyP(4) with $[poly(dAdT)]_2$ (Figure 6c) and $[poly(dGdC)]_2$ (Figure 6d) obtained by using 457.9-nm excitation ($R = 0.01$), the most obvious change upon addition of these polymers was the disappearance of the peaks at ca. 1354, 1454, and 1558 cm^{-1} of the six-coordinate species. Note that any small amount of six-coordinate species present would have been selectively enhanced at this excitation wavelength. Addition of CT DNA, poly(U), or poly(dU) at $R = 0.01$ gave a spectrum very similar to that found on addition of $[poly(dGdC)]_2$, suggesting a complete conversion to four-coordinate species. A titration with poly(U) showed that the disappearance of the six-coordinate species was very abrupt; the Raman spectrum of NiTMpyP(4) remained essentially unchanged with the addition of poly(U) for R up to 0.225. Only for $R = 0.2$ or less did the six-coordinate species disappear completely.

Addition to NiTMpyP(4) of the four anionic non-DNA polymers, dextran sulfate, phosvitin, heparin, and poly(D-glutamic acid), gave spectra indicative of different mixtures of four- and six-coordinate species. Figure 7 shows the Raman spectra of NiTMpyP(4) with the four polymers between 1150 and 1700 cm^{-1} with 457.9-nm excitation at low R values of ca. 10^{-4}. In a titration, dextran sulfate caused a complete conversion to the four-coordinate form at low R values. The shift, however, was not abrupt as with poly(U); a gradual shift from six-coordinate to four-coordinate forms started at $R = 0.5$ and was complete at $R = 0.1$. A small amount of six-coordinate species remained with phosvitin and somewhat more with heparin. Poly(D-glutamic acid) caused the smallest increase in the four-coordinate species.

There were other changes in the Raman spectrum of NiTMpyP(4) upon addition of the polymers, especially with dextran sulfate and $[poly(dAdT)]_2$. Addition of dextran sulfate changed the intensity pattern of the three peaks between 1150 and 1300 cm^{-1} (Figure 7). While the intensity of the peak at ca. 1192 cm^{-1} remained unchanged as compared to the other peaks, that at ca. 1220 cm^{-1} was greatly reduced and broadened and that at ca. 1255 cm^{-1} was enhanced. These three peaks had been assigned to the pyridyl ring and/or the attachment of the pyridyl

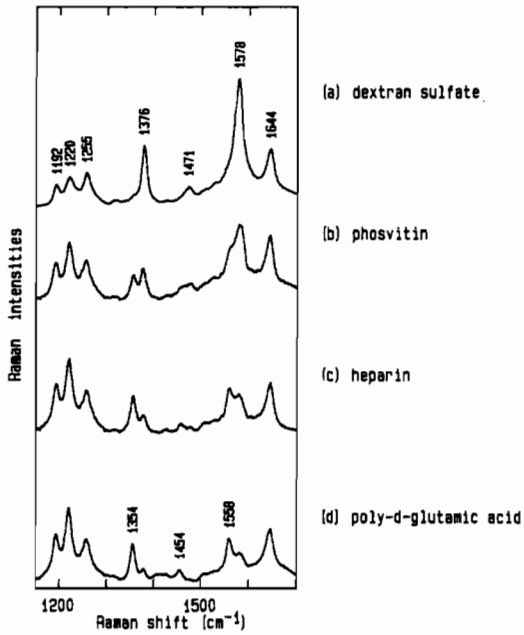

Figure 7. Raman spectra of NiTMpyP(4) with dextran sulfate (a), phosvitin (b), heparin (c), and poly(D-glutamic acid) (d). Samples (4 × 10^{-5} M) were at ambient temperature, in 0.01 M NaCl (pH 7.0). Excitation was 457.9 nm. A smooth background has been subtracted for each spectrum.

ring to the porphyrin.[25] In the titration with dextran sulfate, the intensity pattern change required a very low $R = 0.01$, whereas the disappearance of the bands of the six-coordinate species was complete even at $R = 0.1$. Similar intensity pattern changes were observed with the addition of $[poly(dAdT)]_2$ but not with the other polymers studied. It is noteworthy that the intensity change can be detected only with 457.9-nm excitation.

In addition, there were some frequency changes in the two peaks at ca. 1003 and 1097 cm^{-1} with the addition of the nucleic acid polymers. With 457.9-nm excitation, the sharp peak at 1003 cm^{-1} was shifted to 1014, 1014, and 1004 cm^{-1} upon addition of $[poly(dAdT)]_2$, poly(U), and $[poly(dGdC)]_2$, respectively (cf. Figure 6). Indeed, the relative intensity of this peak compared to that of the ca. 1097-cm^{-1} peak was very similar to that of NiTMpyP(4) in 50% acetone when only four-coordinate nickel was present (data not shown). This was not surprising, since only the four-coordinate species was present. However, changes in the 1097-cm^{-1} peak were more complicated. Upon addition of $[poly(dGdC)]_2$ and all other nucleic acid polymers studied except $[poly(dAdT)]_2$, the peak remained relatively sharp and shifted by about 10 cm^{-1} depending on the polymer, whereas upon addition of $[poly(dAdT)]_2$ the peak split into two overlapping bands at ca. 1102 and ca. 1114 cm^{-1}. Similar splitting of this peak had been observed previously by using 406.7-nm excitation and higher salt concentration (0.2 M NaCl).[26]

We point out that the combination of an intensity pattern change in the region between 1150 and 1300 cm^{-1} and a splitting of the 1097-cm^{-1} peak was observed only with the addition of $[poly(dAdT)]_2$ (with 457.9-nm excitation). Dextran sulfate at low R ($\sim 10^{-4}$) can induce only the intensity pattern change. The 1097-cm^{-1} peak was relatively sharp at $R = 0.01$. At lower R values, the peak seemed to remain sharp, but there was interference due to a broad dextran sulfate peak at ca. 1060 cm^{-1}. At low R values of the other three anionic polymers, the spectra contained a sharp 1097-cm^{-1} peak but also had an interfering peak of varying intensity at ca. 1060 cm^{-1}.

Because of the interesting differences in the optical and CD spectra of NiTMpyP(4) for low and high salt conditions upon addition of $[poly(dAdT)]_2$, the corresponding Raman spectra were recorded with both 406.7- and 457.9-nm excitation. At high R values, in contrast to the differences in the optical and CD spectra, there was no significant difference in the Raman spectra under both salt conditions. Some conversion of six- to four-coordinate species can be seen with both salt conditions. At $R = 0.25$, no six-coordinate species was present at 0.01 M NaCl, but a substantial amount of six-coordinate species still remained at 0.2 M NaCl. The six-coordinate species disappeared completely at R values below 0.15 under high salt conditions. In contrast, the band at ca. 1097 cm^{-1} was clearly broadened at $R = 0.25$ for both salt conditions, although the CD spectra were very different.

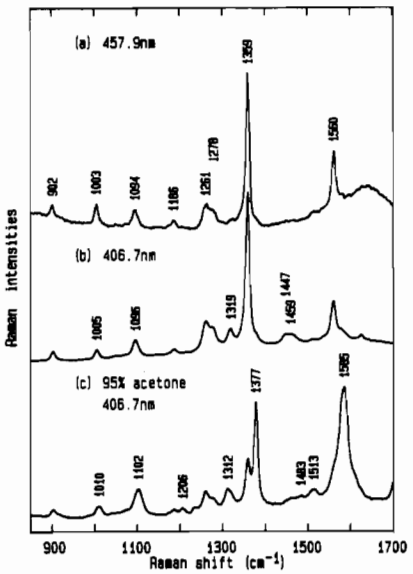

Figure 8. Raman spectra of NiTMpyP(2) in 0.01 M NaCl (pH 7.0), with 457.9- (a) and 406.7-nm (b) excitation and in 95% acetone by volume with 406.7-nm excitation (c). Samples were at ambient temperature with concentrations of 0.03, 0.03, and 0.06 mM, respectively. A smooth background has been subtracted for each spectrum.

Figure 8 shows typical Raman spectra of NiTMpyP(2) in 0.01 M NaCl between 850 and 1700 cm^{-1} using 457.9- and 406.7-nm excitations and in 95% acetone with 406.7-nm excitation. As expected, large differences in the spectral features of NiTMpyP(2) and NiTMpyP(4) were observed for modes due to the pyridiniumyl moieties in the region between 1150 and 1300 cm^{-1}. In addition, the relatively strong pyridyl deformation mode at 1644 cm^{-1} for NiTMpyP(4) is much weaker and downshifted in NiTMpyP(2). The other spectral features are similar to those of NiTMpyP(4). For example, the two core-size-sensitive C_α–C_β and C_β–C_β stretching modes at ca. 1359 and 1560 cm^{-1} are very prominent in both excitations. These peaks are due to the six-coordinate NiTMpyP(2) species that predominates in 0.01 M NaCl solution (Figure 8a,b). In agreement with the visible absorption changes on increasing acetone percentage, there was a gradual decrease in the intensities of the six-coordinate peaks at ca. 1359 and 1560 cm^{-1} and a concomitant increase in the intensities of the four-coordinate peaks at ca. 1377 and 1585 cm^{-1}. In addition, at least two new peaks gradually appeared at 1206 and 1513 cm^{-1}. The intensities of the broad peak around 1447 cm^{-1} and the shoulder at 1278 cm^{-1} also gradually diminished as the percentage of acetone increased (cf. Figures 8b,c). Furthermore, the peak at 1319 cm^{-1} was downshifted to 1312 cm^{-1} and its intensity increased in 95% acetone solution. These smaller changes, which are related to the conversion of the six-coordinate to the four-coordinate species, cannot be observed with 457.9-nm excitation (see Figure 8a) because of the generally lower enhancement at this wavelength and the relatively stronger interfering bands of acetone.

Figures 9 and 10a show the Raman spectra of NiTMpyP(2) with CT DNA, $[poly(dAdT)]_2$, $[poly(dGdC)]_2$, and poly(U) obtained by using 406.7-nm excitation ($R = 0.01$). The extent of the most obvious change, the appearance of the four-coordinate peaks at 1379 and 1587 cm^{-1}, was different for the four nucleic acids. The change ranged from almost complete with $[poly(dAdT)]_2$ to only minor with poly(U). These changes on addition of CT DNA were only slightly smaller than those found with $[poly(dAdT)]_2$, consistent with previous results at high salt.[14] Thus, the amount of four- and six-coordinate species depends on

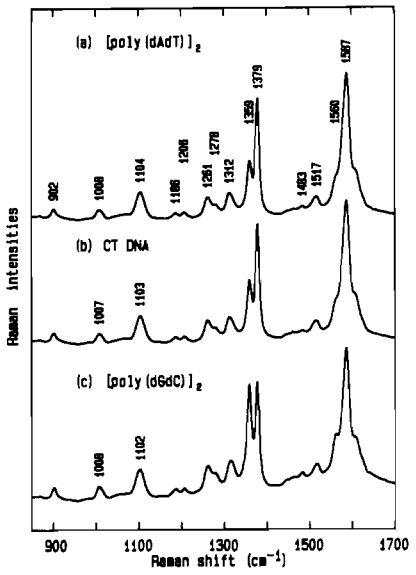

Figure 9. Raman spectra of NiTMpyP(2) with $[poly(dAdT)]_2$ (a), CT DNA (b), and $[poly(dGdC)]_2$ (c). Samples were at ambient temperature, in 0.01 M NaCl (pH 7.0), with NiTMpyP(2) concentrations of 0.027, 0.027, and 0.02 mM, respectively. Excitation was 406.7 nm. A smooth background has been subtracted for each spectrum.

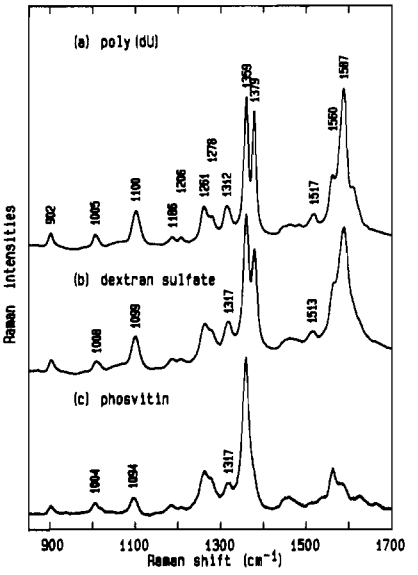

Figure 10. Raman spectra of NiTMpyP(2) with poly(U) (a), dextran sulfate (b), and phosvitin (c). Samples were at ambient temperature, in 0.01 M NaCl (pH 7.0) with NiTMpyP(2) concentrations of 0.03, 0.04, and 0.04 mM, respectively. Excitation was 406.7 nm. A smooth background has been subtracted for each spectrum.

the nature of the DNA polymer, a conclusion corroborated by the behavior of these two core-size-sensitive modes with 457.9-nm excitation (data not shown). In addition, with 406.7-nm excitation, the smaller changes associated with the appearance of four-coordinate species (as described above for acetone) were also observed with the addition of the DNA polymers. For example, there were new peaks at 1206 and 1517 cm^{-1} and reduction in the intensities at ca. 1278 and 1450 cm^{-1} (cf. Figure 9a). In fact, the overall general spectral features of NiTMpyP(2) in the presence of CT DNA or $[poly(dAdT)]_2$ appear nearly identical with those observed in 95% acetone. These changes were also observed but to a lesser extent in the spectra upon addition of $[poly(dGdC)]_2$ and poly(U), indicating that there is less conversion to four-coordinate species.

The effects of two non-DNA anionic polymers on the NiTMpyP(2) Raman spectrum are shown in Figure 10b,c. Addition of poly(D-glutamic acid) and heparin produced minimal to no change in the Raman spectrum of NiTMpyP(2) (data not shown). The porphyrin remained six-coordinate, perhaps with a trace of four-coordinate species with heparin. Addition of phosvitin converted a small amount of six-coordinate NiTMpyP(2) to the four-coordinate form, as seen from the shoulder at 1587 cm^{-1}. A substantial amount of four-coordinate species was observed with the addition of dextran sulfate (cf. the 1379-cm^{-1} peak and the even smaller changes in the weaker four-coordinate peaks at ca. 1206, 1278, 1450, and 1517 cm^{-1}).

Discussion

We recently discovered[10] that porphyrins exhibit considerable inhibition of HIV-1, the RNA virus associated with AIDS, and we wished to assess the binding of other porphyrins to nucleic acids including ribonucleic acids and to other types of polymers. In some cases, such porphyrins are similar to NiTMpyP(4), which has only moderate activity against the HIV-1 virus. It is clearly desirable to extend the utility of resonance Raman spectroscopy using the Ni(II) derivatives to other polymer classes and to determine whether new types of species could be identified. The informative background already available on these porphyrins,[4,16,17] when extended with studies such as those reported here, will lay the foundation for exploring interactions of the porphyrins with viruses by using resonance Raman spectroscopy. Furthermore, we hoped that information on some of the model polymers selected for this study might in turn prove insightful into the previously explored interactions of these porphyrins with DNA duplexes.

Before discussing our findings in detail, it is important to systematize previous findings. The equilibrium between four- and six-coordinate NiTMpyP(4) is finely balanced, and it is not surprising that the environment can influence its position. The effect of acetone may be a mass law effect; i.e., the activity of water is decreased in the mixed-solvent system. Likewise, the activity of water may be altered by the anionic polymer, the structure of the porphyrin ligand may be perturbed by the interaction with the negative groups of the polymers, the porphyrin may bind in a hydrophobic pocket, etc. Perturbed structures could be formed by bound six- or four-coordinate NiTMpyP(4).

Nakamoto and co-workers found that four-coordinate forms are greatly favored when the porphyrin bound to duplex DNAs.[23] Furthermore, although small shifts in the Raman bands were observed, the structural perturbations were usually minimal. However, a clearly perturbed four-coordinate species was found with $[poly(dAdT)]_2$.

We systematize these findings and our findings in the following scheme.

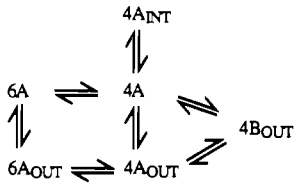

In this scheme, 6 and 4 designate six- and four-coordinate forms, respectively. A designates an essentially unperturbed porphyrin whereas B represents a significantly perturbed porphyrin. By significant perturbation, we mean that the resonance Raman bands exhibit a unique pattern different from those found normally. The subscripts, INT and OUT, indicate polymer-bound species that interact through intercalative or outside, possibly groove-bound modes, respectively. Thus, for example, $4B_{OUT}$ is the perturbed species formed when NiTMpyP(4) binds to $[poly(dAdT)]_2$.

With this scheme, we can specify our goals in this study. First, we wished to determine whether significant percentages of $6A_{OUT}$ could exist bound to a polymer. Second, we wanted to assess whether $4B_{OUT}$ could be formed with other polymers or whether related species could be formed by other polymers. Third, we hoped to discover if $4A_{OUT}$ could exist bound to non-DNA polymers. Fourth, we wished to evaluate the use of nickel porphyrins as a means for classifying polymers.

Indeed, the new spectroscopically distinct behavior observed in our studies with poly(dU), poly(U), and dextran sulfate provided

some useful insight into the existence of $6A_{OUT}$ (our first goal). The principal evidence is the presence of both four- and six-coordinate peaks at diminished intensity in the Soret region at high R values (Figures 2 and 3). This decrease indicates that both forms are bound to the polymers, but that the equilibrium position is not greatly changed. This intensity decrease was followed by a very sharp conversion to a single weak Soret band and subsequently by the increase in intensity of this remaining band at lower R values.

The CD results are consistent with polymer binding at both high and low R values. At low R values, a negative induced CD band is present for both dextran sulfate and poly(U). This band has been attributed to an intercalated species,[28] but neither polymer studied here has intercalation sites. The results with poly(U) at high R are most informative. There are two bands, a result consistent with the presence of both $6A_{OUT}$ and $4A_{OUT}$ species.

The resonance Raman results are consistent with the presence of a $6A_{OUT}$ species. The differences in the concentration dependence of six- to four-coordination conversion, which occurred abruptly for poly(U) and gradually for dextran sulfate, were also observed in both the optical and Raman studies. The detection of a $6A_{OUT}$ species suggests that it may be possible to use resonance Raman spectroscopy to distinguish porphyrin species bound to single-stranded regions of nucleic acid from those bound to duplex regions.

A second goal was to determine if a unique $4B_{OUT}$ species, described by Nakamoto's laboratory,[23] could be found with other polymers. The unique species was found when NiTMpyP(4) interacted with $[poly(dAdT)]_2$. The 1097-cm^{-1} band was split into two bands upon addition of $[poly(dAdT)]_2$ in 0.2 M NaCl. This indicates that there are two major subgroups for this mode, which has been assigned to $\delta(C_\beta\text{–H})$.[25] With 457.9-nm excitation and 0.01 M NaCl, not only have we observed this splitting but we also observed changes in the intensity pattern of the three peaks between 1150 and 1300 cm^{-1}. These three modes are related to the pyridyl group and its attachment to the porphyrin core. The band at 1220 cm^{-1} is substantially broadened and may be due to a combination of two peaks. It is not clear why these intensity changes can be observed only with 457.9-nm excitation. It does, however, indicate a specific interaction of the pyridyl ring with the $[poly(dAdT)]_2$ polymer upon complex formation. On the basis of a conservative type CD spectrum of NiTMpyP(4)–$[poly(dAdT)]_2$ at $R < 0.03$ in phosphate buffer (0.2 M ionic strength), Pasternack[28] suggested that there may be two types of binding. The positive CD component is due to groove-binding while the negative component is possibly due to either partial intercalation or stacked aggregation along isolated regions. The splitting of the 1097-cm^{-1} peak and the broadening of the 1220-cm^{-1} peak are consistent with the existence of two types of binding. The details of such binding remain unclear.

Our CD results at 0.01 M NaCl reveal a new type of conservative signal at high R (Figure 5). This new CD spectrum suggests that extensive stacking may occur along the polymer since its maximum value was observed at ca. $R = 0.4$, a value at which the porphyrins should be closely stacked along the helix. The Raman results indicate that the unique $4B_{OUT}$ species is present when we observe this strong CD feature. On the other hand, at low R values where the inverted conservative-like CD signal was observed, the splitting of the 1097-cm^{-1} band, characteristic of $4B_{OUT}$, was also observed. Of some interest, when the CD spectrum was monitored in 0.2 M NaCl, we did not find the new strong conservative CD signal we found at lower salt concentration. Under high salt conditions, the splitting of the 1097-cm^{-1} band was reported even at high R values,[23] and we have confirmed this finding. Furthermore, we note that the 1220-cm^{-1} band is broadened. The presence of $4B_{OUT}$ from the initiation of the titration under both salt conditions suggests that the CD results are not exclusively indicative of binding mode in isolation but are obviously influenced by the spatial relationships of the porphyrins to each other along the duplex, especially at high R.

Note that the $4B_{OUT}$ species also exhibited an altered intensity pattern in the 1150–1300-cm^{-1} region. It is interesting that addition of dextran sulfate also produced the intensity changes in the 1150–1300-cm^{-1} region, but the peak at 1097 cm^{-1} remained sharp, suggesting that the two types of spectral changes are independent. On the basis of our findings, it does appear that the binding to the weak $[poly(dAdT)]_2$ duplex induces a species that may only exist in this type of environment. Apparently, dextran sulfate can induce some changes in the porphyrin structure or electronic properties that have some features of $4B_{OUT}$, but the porphyrin structure in this case must be considered to be relatively unperturbed.

The implications of this finding are interesting. Many studies have revealed that $[poly(dAdT)]_2$ binds outside binding porphyrins more favorably than $[poly(dGdC)]_2$.[12] The explanation typically offered for this phenomenon is that the greater flexibility of the $[poly(dAdT)]_2$ polymer allows the polymer to distort in such a way as to bring the positively charged moieties into close proximity to negatively charged phosphate groups in the backbone.[4,16,17] The unique species appears to reflect this flexibility, but the changes in the Raman spectrum have been attributed to a distortion in the porphyrin induced by the duplex,[23] which is itself distorted. Our results with poly(dU), poly(U), and dextran sulfate are consistent with this interpretation. Thus, the flexible polymers we have investigated probably fully distort to accommodate the porphyrin geometry, leading to no unusual changes in the porphyrin Raman spectrum. If this explanation, which requires more investigation, is correct, it is conceivable that resonance Raman spectroscopy combined with visible spectroscopy may allow us to distinguish not only between binding to single-stranded and double-stranded regions but also between readily distortable and less distortable duplex regions. Thus, it appears that $4A_{OUT}$ can exist with several classes of polymers (our third objective) but that formation of $4B_{OUT}$ requires special interactions such as those with the minor groove in weakly stacked, distortable duplex regions of DNA polymers.

On the basis of the spectroscopic results, it is of some interest to classify the diverse polymers we have used (our fourth goal). The local environment of the binding site(s) of the NiTMpyP isomers determines the amount of each coordination form. The strength of the binding constant is also important. The classification is complicated by the possibility of intercalative binding of the NiTMpyP(4) isomer to CT DNA and to $[poly(dGdC)]_2$. However, this problem can be circumvented by using data for NiTMpyP(2), which cannot intercalate. For outside binding, the strength of the binding tends to reflect the flexibility of the polymer. Furthermore, we use the lowest ratios to ensure the greatest extent of binding for our classification scheme. The relative amount of each coordination form can then be used to classify the polymer.

Of all the polymers studied, the weakest binding sites for NiTMpyP(4) are in poly(D-glutamic acid), followed by heparin and then by phosvitin (cf. Figure 7). Unfortunately, NiTMpyP(4) cannot be used to distinguish all the other polymers because only the four-coordinate species can be observed with the addition of the other polymers.

As expected from the lower basicity of the porphyrin ligand,[38] NiTMpyP(2) has a much stronger preference for the six-coordinate species. In our Raman studies, 50% acetone converted all the six-coordinate into four-coordinate species in NiTMpyP(4), but NiTMpyP(2) retains some of the six-coordinate species even in 95% acetone. All major changes observed in the Raman spectrum of NiTMpyP(2) upon addition of acetone or of the polymers are caused by a change in the relative amount of four- and six-coordinate species (Figures 8–10). As for NiTMpyP(4), the relative amount of the two coordination forms of NiTMpyP(2) is an indication of the relative strength of the binding sites of the polymers. From the results in Figures 6, 7, 9, and 10, the order in Table II can be established. Note that both of the nickel porphyrins are needed to establish this order since only six-coordinate NiTMpyP(2) was found with heparin and poly(D-glutamic acid). This result is also consistent with the visible absorption studies.

Table II: Order of Effectiveness of the Polymers in the Conversion of Six- to Four-Coordinate Species

polymer	NiTMpyP(4)	NiTMpyP(2)
most effective		
$[poly(dAdT)]_2$	all four[a]	mostly four[c]
CT DNA	all four	mostly four[c]
$[poly(dGdC)]_2$	all four[a]	mostly four[c]
poly (U)	all four	mostly four[d]
dextran sulfate	all four[b]	mostly four[d]
phosvitin	mostly four[b]	four ≈ six[d]
heparin	mostly four[b]	all six
poly(D-glutamic acid)	mostly four[b]	all six
less effective		

[a] See Figure 6. [b] See Figure 7. [c] See Figure 9. [d] See Figure 10.

In conclusion, resonance Raman spectroscopy could be very valuable in assessing the binding of such porphyrins to viruses and other well-defined nucleic acids as well as to proteins. Such studies are planned. The special characteristics found for the NiTMpyP(4) interaction with $[poly(dAdT)]_2$ appear to be relatively unique and are not reproduced even with flexible single-stranded nucleic acids. At high R values, such nucleic acids appear to interact with an outside-bound, six-coordinate form of NiTMpyP(4). However, a relatively unperturbed four-coordinate form of NiTMPyP(4) appears to be the most common polymer-bound form, regardless of the nature of the polymer.

Acknowledgment. This work was supported by NIH Grant AI 27196 to L.G.M. and Grant GM 38555 to K.T.Y. We thank the National Institutes of Health for an instrument grant to purchase the CD spectropolarimeter.

Registry No. NiTMpyP(4), 48242-71-3; NiTMpyP(2), 128235-51-8; poly(dU), 35297-30-4; poly(U), 27416-86-0; $[poly(dAdT)]_2$, 26966-61-0; $[poly(dGdC)]_2$, 36786-90-0; Ni, 7440-02-0; NaCl, 7647-14-5; dextran sulfate, 9042-14-2; heparin, 9005-49-6; poly(D-glutamic acid), 25104-13-6; poly(D,L-glutamic acid) SRU, 27030-24-6.

Contribution from the Institute of Chemistry, University of Wrocław, 14 F. Joliot-Curie St., Wrocław 50 383, Poland, and Institute of General Chemistry, I-17, Technical University of Łódź, Łódź 90 924, Poland

Reactions of the Iron(III) Tetraphenylporphyrin π Cation Radical with Triphenylphosphine and the Nitrite Anion. Formation of β-Substituted Iron(III) Porphyrins

Andrzej Małek,[†] Lechosław Latos-Grażyński,*[,†] Tadeusz J. Bartczak,[‡] and Andrzej Żądło[‡]

Received September 26, 1990

The formation of iron(III) β-(triphenylphosphonio)tetraphenylporphyrin (β-PPh_3^+-TPP)Fe^{III} and iron(III) β-nitrotetraphenylporphyrin (β-NO_2-TPP)Fe^{III} in the reaction of iron(III) tetraphenylporphyrin cation radical (TPP$^{\bullet}$)$Fe^{III}(ClO_4)_2$ with triphenylphosphine or nitrite anion has been established through a variety of spectroscopic investigations. The reaction mechanism seems to be analogous to that elucidated for a variety of metalloporphyrin cation radicals or arene cation radicals. The structure of (β-PPh_3^+-TPP)$Fe^{III}Cl_2 \cdot CHCl_3$, $C_{63}H_{43}N_4Cl_5PFe$, has been determined at 173 K by X-ray diffraction: monoclinic space group $I2/a$, $Z = 8$, $a = 27.948$ (3) Å, $b = 11.286$ (3) Å, $c = 33.633$ (5) Å, $\beta = 94.31$ (1)°, least-squares refinement of parameters using 3658 reflections (Mo Kα) yielding $R = 0.091$, $R_w = 0.06$. The structural study of (β-PPh_3^+-TPP)$Fe^{III}Cl_2$ revealed its "zwitterionic" nature. The species belongs to a rather small class of high-spin six-coordinate iron(III) porphyrins and is the first example where two apical positions are occupied by chloride anions. The Fe–Cl distances are Fe–Cl(1) = 2.429(3) Å and Fe–Cl(2) = 2.348 (3) Å. The iron atom is precisely located in the plane of an expanded porphyrin core of a saddlelike conformation with mean Fe–N = 2.055 (7) Å. This value is in the range of Fe–N distances found in other known high-spin ferric porphyrins. This geometry is also preserved in chloroform and has been established for bromide and iodide axial ligands. The proton NMR spectra of high-spin and low-spin iron(III) β-substituted porphyrins have been obtained and analyzed. Functional group assignments have been made with the use of selective deuteration and methyl substitution. The pattern of seven pyrrole resonances reflects the asymmetry that results from β-substitution. This pattern is diagnostic for mono-β-substitution. Because of hindrance of the phenyl group, rotation around the pyrrole carbon–phosphorus bond is restricted.

Introduction

One-electron oxidation of iron(III) porphyrins produces either iron(IV) porphyrins or iron(III) porphyrin cation radicals. Intense interest in these compounds has been stimulated by their involvement in various biological processes[1-3] or in catalytic reactions of metalloporphyrins.[4-6] Their electronic structures and spectroscopic and magnetic properties have been elaborated in detail.[7-14] The magnetic interaction between iron and the radical form of the macrocyclic ligand has been related to the porphyrin core structure.[10] A relationship between the pattern of *meso*-phenyl resonances and the nature of magnetic coupling (ferro- vs antiferromagnetic) has been established.[10,15] Imidazole ligands convert the high-spin iron(III) porphyrin cation-radical complexes to low-spin iron(III) porphyrin cation-radical complexes. Addition of imidazole also induces a reduction of iron(III) porphyrin cation-radical complex to the corresponding low-spin iron(III) porphyrin.[12]

Despite the numerous structural investigations, the reactivity of iron(III) porphyrin cation-radical complexes has received little

[†] University of Wrocław.
[‡] Technical University of Łódź.

(1) (a) Dunford, H. B.; Stillman, J. S. *Coord. Chem. Rev.* **1976**, *19*, 187. (b) Dunford, H. B. *Adv. Inorg. Biochem.* **1982**, *4*, 41.
(2) Hewson, W. D.; Hage, L. P. *The Porphyrins*; Dolphin, D., Ed.; Academic Press: New York, 1979; Vol. 7, pp 295–332.
(3) Dawson, J. *Science* **1988**, *240*, 433.
(4) McMurry, J. T.; Groves, J. T. In *Cytochrome P-450: Structure, Mechanism and Biochemistry*; Ortiz de Montellano, P. R., Ed.; Plenum Press: New York, pp 1–27.
(5) Bruice, T. C. in *Mechanistic Principles of Enzyme Activity*; Liebman, J. F., Greenberg, A., Eds.; VCH Publisher Inc.: New York, 1988; pp 227–277.
(6) Arasasingham, R.; Balch, A. L.; Latos-Grażyński, L. In *The Role of Oxygen in Chemistry and Biochemistry*; Ando, W., Moro-Oka, Y., Eds.; Studies in Organic Chemistry 33; Elsevier: New York, 1988; p 417.
(7) Gans, P.; Marchon, J.; Reed, C. A. *Nouv. J. Chim.* **1981**, *5*, 203.
(8) Buisson, G.; Deronizer, A.; Duée, E.; Gans, P.; Marchon, J. C.; Regnard, J. R. *J. Am. Chem. Soc.* **1982**, *104*, 6793.
(9) Scholz, W. F.; Reed, C. A.; Scheidt, R. W.; Lee, Y. J.; Lang, G. *J. Am. Chem. Soc.* **1982**, *104*, 6791.
(10) Gans, P.; Buisson, G.; Duée, E.; Marchon, J.-C.; Erler, B. S.; Scholz, W. F.; Reed, C. A. *J. Am. Chem. Soc.* **1986**, *108*, 1223.
(11) Phillippi, M. A.; Goff, H. M. *J. Am. Chem. Soc.* **1982**, *104*, 6026.

0020-1669/91/1330-3222$02.50/0